

Dislocation structures in deformed CoO and MnO

K. C. GORETTA, R. E. COOK, J. L. ROUTBORT

Materials Science Division, Argonne National Laboratory, Argonne, Illinois 60439, USA

Transmission electron microscopy (TEM) and etch-pitting techniques have been used to examine dislocation structures of CoO and MnO single crystals deformed into steady state from 1000 to 1400°C. In this temperature range, studies have shown that there are low- and high-temperature activation energies (Q) and stress exponents (n). No change was observed in the structures of samples deformed within this temperature range. It is concluded, therefore, that any change in Q and n values is due to a change in oxygen diffusion path from the bulk at higher temperatures to along dislocation cores at lower temperatures, rather than being due to a change in the rate-controlling mechanism of deformation

1. Introduction

Cation-deficient NaCl-structured oxides such as CoO and MnO are ideal materials for the study of intrinsic properties. Small impurity concentrations generally affect properties of stoichiometric ceramics substantially, whereas for nonstoichiometric oxides with sufficiently large deviations from stoichiometry (δ) impurity concentrations are much smaller than vacancy concentrations, and hence impurities have little effect. Values of δ depend on temperature (T) and oxygen partial pressure (p_{O_2}).

The high-temperature deformation behaviour of CoO [1-3] and MnO [4, 5] has been shown to be dependent on T and δ . In both oxides, steady-state deformation is governed by recovery via dislocation climb [1-4, 6], the rate of which is controlled by diffusion of oxygen [7]. Oxygen diffusion occurs by vacancy motion for small δ and by interstitial motion for large δ [3]. The steady-state strain rate ($\dot{\epsilon}$) is given by

$$\dot{\epsilon} \propto \tau_s^n \exp - (Q/RT),$$

where τ_s is the steady-state resolved shear stress [3].

For CoO from 1000 to 1400°C, two studies [2, 3] show Q to decrease with decreasing temperature and in one study [2], the value of n for $T \geq 1200^\circ\text{C}$ increases to $n + 2$ as T decreases to 1000°C. Some data from other studies are in agreement with the increase in n [1], others are not [8]. It has been suggested that a change in diffusion path or in the rate-controlling diffusing species may account for the observed differences in Q and n [2].

In MnO, the situation is similar, but more consistent. For $T \geq 1150^\circ\text{C}$, Q has been found to be $470 \pm 80 \text{ kJ mol}^{-1}$ in the regime of oxygen-vacancy control of deformation and $410 \pm 80 \text{ kJ mol}^{-1}$ in the regime of oxygen-interstitial control. For $T \leq 1000^\circ\text{C}$, however, Q was found to be $200 \pm 50 \text{ kJ mol}^{-1}$ [9]. Additionally, in both regimes, the high-temperature value of n reaches $n + 2$ for $T \leq 1000^\circ\text{C}$ [10].

A change in path of the oxygen, from volume diffusion to pipe diffusion along dislocation cores, could result in a substantial decrease in Q and cause n to increase to $n + 2$ [11]. It is also possible, however, that changes in Q and n could be caused by a change from climb control of deformation to glide control [12]. A change in diffusion path should not affect dislocation structures appreciably, but a change from climb to glide control should. Such a change to glide control of high-temperature deformation has been observed in the isostructural oxide NiO [12, 13]. For this oxide, substantial differences in dislocation structures have been observed between the two rate-controlling mechanisms [13, 14].

The objective of this investigation was to determine whether the observed differences in Q and n values with temperature induce differences in dislocation structure. Structures in CoO and MnO which were deformed from 1000 to 1400°C have been examined by TEM and etch pitting. It will be shown that no change in structure occurs, and therefore observed differences in Q and n values are probably due to changes in oxygen diffusion path: bulk diffusion predominates at higher temperatures and diffusion along dislocation cores predominates at lower temperatures.

2. Experimental procedures

Details concerning the growth and deformation of the CoO and MnO single crystals have been described [3-5]. Sections for TEM specimens were cut from the centre of a given sample along either the $\{100\}$ plane perpendicular to the load axis or along a $\{110\}$ plane parallel to a slip direction. Discs of 2.6 mm diameter were cut from each section. The discs were mechanically polished to a thickness of about 130 μm , and then a VCR Group Dimpler (San Francisco, California) was used to polish the centre of each disc to a minimum dimension of about 30 μm . Each disc was then ion-beam milled with argon until perforation

occurred. Average milling parameters were $30 \mu\text{A}$ and 5 kV , with milling occurring at 20° angles of incidence.

Specimens for etch pitting were cut along $\{100\}$ planes perpendicular to the load axis and were mechanically polished to a finish of $0.3 \mu\text{m}$. For CoO, an etching procedure used by Castaing and Dominguez-Rodriguez was followed [15]: specimens were immersed for approximately 30 min in a quiescent mixture of 100 ml distilled water, 40 ml concentrated HNO_3 and 40 ml concentrated HF. For MnO, etching was achieved by immersion for 20 sec in a mixture of 150 ml distilled water, 12 ml concentrated HF and 2 ml HNO_3 . Neither etching procedure was completely effective: not all regions of the samples etched, and spinel-structured precipitates which formed upon cooling [16] etched strongly, which made it impossible to determine dislocation densities by etch pitting. Well-etched areas were photographed, and subgrain sizes were measured. Reported subgrain sizes (D) represent averages of between 10 and 30 individual subgrain measurements.

3. Results and discussion

3.1. TEM observations

Several CoO samples were examined by TEM. The range of temperature for deformation was 1000 to 1200°C , the range of p_{O_2} was 10^{-6} to 10^5 Pa . No obvious differences in dislocation structures were observed between any of the samples. In all samples, subgrain boundaries characteristic of those formed by dislocation climb were the dominant features.

A few three-dimensional boundaries consisting of hexagonal arrays were observed, as shown in Fig. 1. This sample was deformed at 1200°C at a p_{O_2} for which oxygen vacancies controlled deformation. All

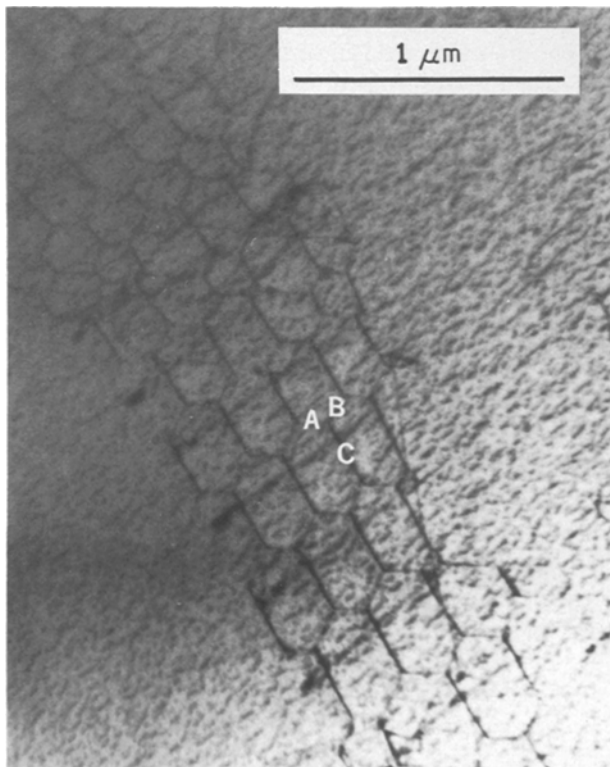


Figure 1 Three-dimensional dislocation network in CoO, deformed at 1200°C , $p_{\text{O}_2} = 10^{-4} \text{ Pa}$, $\dot{\epsilon} = 5 \times 10^{-5} \text{ sec}^{-1}$, $\epsilon = 0.11$.

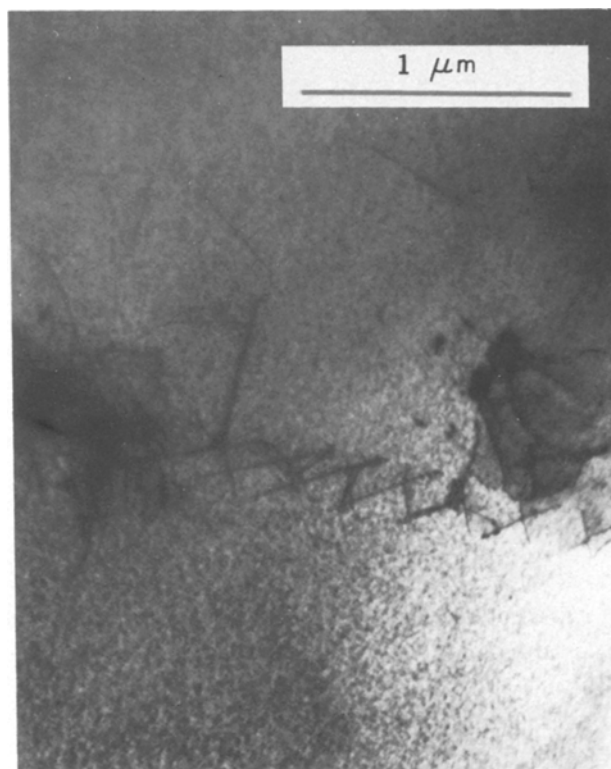


Figure 2 Subgrain boundary in CoO, deformed at 1200°C , $p_{\text{O}_2} = 10^{-4} \text{ Pa}$, $\dot{\epsilon} = 5 \times 10^{-5} \text{ sec}^{-1}$, $\epsilon = 0.09$.

of the dislocations are in contrast in this figure. Use of the $\mathbf{g} \cdot \mathbf{b} = 0$ criterion for dislocations going out of contrast showed that the segments of a node had the following Burgers vectors: $A = a_0/2 [10\bar{1}]$, $B = a_0/2 [0\bar{1}1]$, $C = a_0/2 [\bar{1}10]$, where C was determined to be a screw dislocation. The second type of subgrain boundary consisted of parallel edge dislocations for

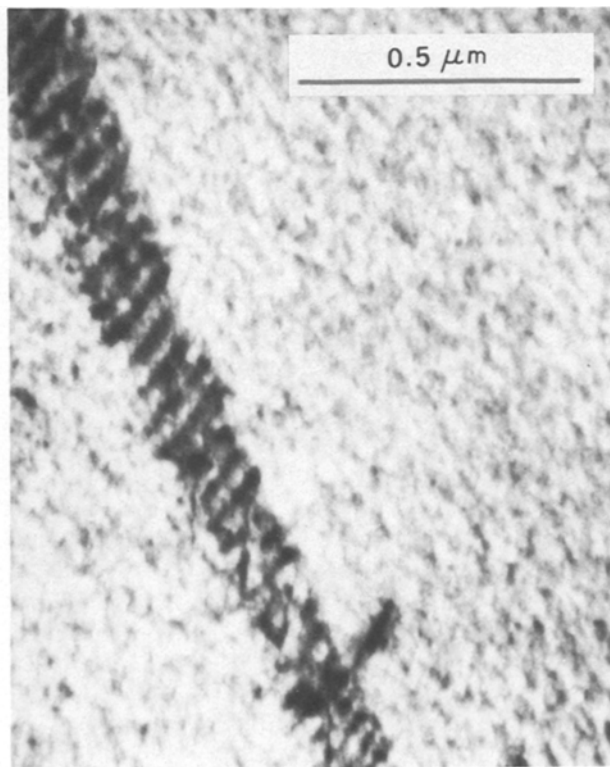


Figure 3 Subgrain boundary in MnO, deformed in creep at 1000°C , $p_{\text{O}_2} = 10^{-8} \text{ Pa}$, $\tau_c = 16.2 \text{ MPa}$, $\epsilon = 0.18$.

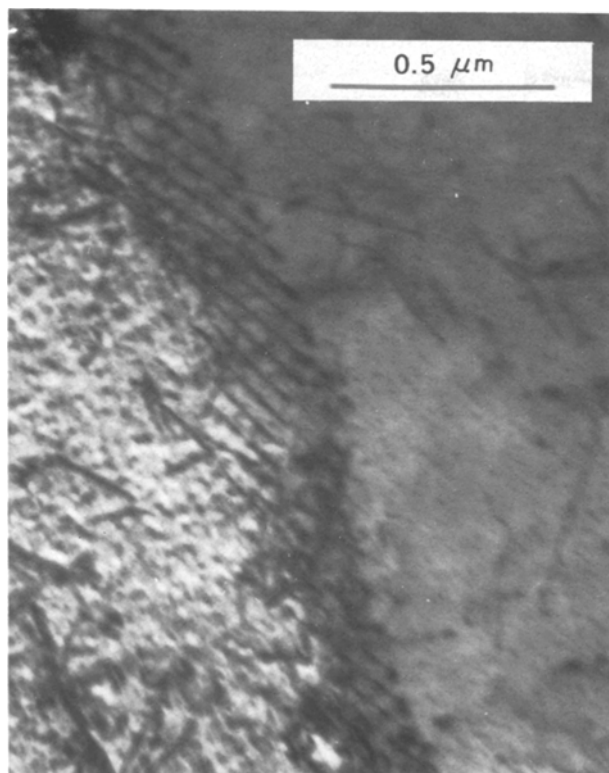


Figure 4 Subgrain boundary in MnO, deformed at 1200°C, $p_{O_2} = 1 \text{ Pa}$, $\dot{\epsilon} = 5 \times 10^{-5} \text{ sec}^{-1}$, $\epsilon = 0.12$.

which the $\mathbf{g} \cdot \mathbf{b} = 0$ criterion suggests that the Burgers vector was also $a_0/2 [110]$ (Fig. 2).

Both types of subgrain boundaries were observed in all samples examined and have been observed by other investigators in CoO deformed at 1000°C in a regime of oxygen-interstitial control of deformation [1, 6, 17]. Therefore, although values of Q and n may change with T (or possibly as a function of δ [10]) neither T nor δ had any effect on dislocation structures over the ranges examined.

Eight MnO samples were examined by TEM. Deformation parameters varied substantially among the samples: $1000^\circ \text{C} \leq T \leq 1400^\circ \text{C}$, $10^{-8} \text{ Pa} \leq p_{O_2} \leq 10^2 \text{ Pa}$, total strain from 2 to 35%. All subgrain boundaries observed consisted of two-dimensional arrays of parallel edge dislocations; no three-dimensional boundaries were observed (Figs 3 and 4). As was the case for CoO, neither T nor δ had

an effect on dislocation structure. It is thus strongly suggested that changes in Q and n values reflect a change in the diffusion path of oxygen because a change from climb to glide control of deformation would give rise to different structures.

3.2. Etch-pit studies

Most models of steady-state deformation predict that subgrain size, D , should be proportional to τ_s^{-1} [18]. However, many studies find

$$D \propto \tau_s^{-k}$$

where k ranges from 0.6 to 1.0 [19]. If D has the same functional relationship to τ_s for all temperatures from 1000 to 1400°C, then it seems likely that no change in deformation mechanism occurs over this temperature range.

For CoO, deformed samples covering a range of temperature from 1000 to 1400°C and a range of p_{O_2} from 10^{-4} to 10^4 Pa were selected for etch pitting. Results of $\log D$ against $\log \tau_s$ are shown in Fig. 5 (data points from another study [15] are shown for comparison). A least-squares fit to the data yielded $D \propto \tau_s^{-0.7}$ and no discontinuity was present above or below 1200°C.

For MnO, only samples deformed at 1000°C were etched. This choice was made because the etching procedure used was not as effective in MnO as in CoO so that only relatively small subgrains could be measured reliably. It was also found that $D \propto \tau_s^{-0.7}$ (Fig. 6). Therefore, both MnO and CoO exhibit the same functional dependence of D on τ_s , which again tends to confirm that changes in Q and n values arise from changes in oxygen diffusion path as temperature changes.

Although it is often predicted that pipe diffusion down dislocation cores should dominate below some temperature (usually about 0.6 of the melting temperature [11]) pipe diffusion has not previously been documented in a cation-deficient NaCl-structured oxide. In CoO and MnO, steady-state structures and the relationship between D and τ_s remain constant from 1000 to 1400°C, despite changes in Q and n values. Constant structure implies a single rate-controlling mechanism of deformation. It is inferred, therefore, that observed changes in Q and n values

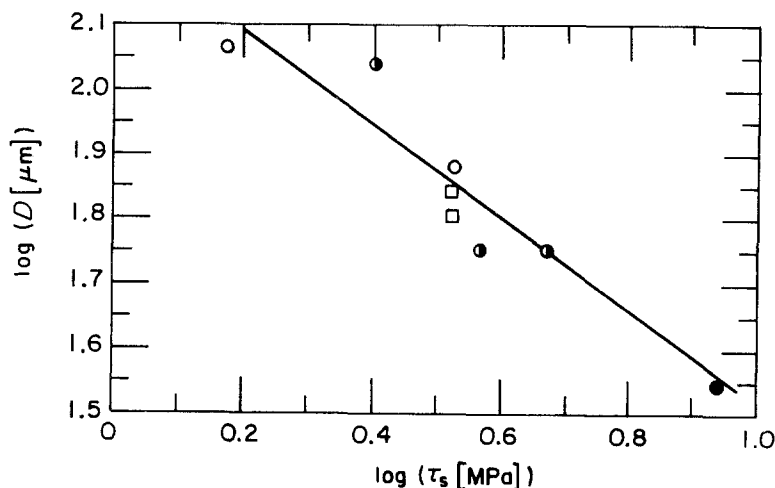


Figure 5 Subgrain size plotted against steady-state stress in CoO. (●) $T = 1000^\circ \text{C}$; (◐) $T = 1200^\circ \text{C}$; (○) $T = 1400^\circ \text{C}$; (□) Castaing and Domguez-Rodríguez [15].

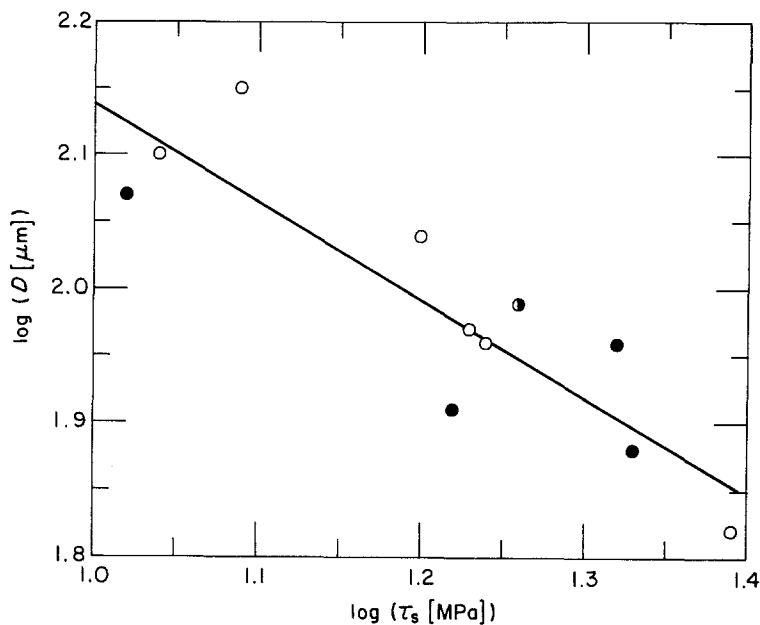


Figure 6 Subgrain size plotted against steady-state stress in MnO at 1000°C. (●) $p_{O_2} = 10^{-5}$ Pa; (◼) $p_{O_2} = 10^{-6}$ Pa; (○) $p_{O_2} = 10^{-8}$ Pa.

arise because oxygen diffusion occurs in the bulk at higher temperatures and along dislocation cores at lower temperatures.

4. Conclusion

For temperatures of 1000 to 1400°C, neither CoO nor MnO exhibits a difference in dislocation structure with either temperature or δ . Climb of edge dislocations controls of deformation rates. Data from deformation studies suggest that a change from volume diffusion of oxygen to pipe diffusion along dislocation cores occurs as temperature falls from about 1200°C to 1000°C. Slight differences exist in subgrain boundaries between CoO and MnO, but both seem typical of a climb-controlled process. For both oxides it was found that $D \propto \tau_s^{-0.7}$.

Acknowledgements

The authors wish to thank Dr C. L. Wiley and G. J. Talaber for growing the single crystals used in this study and J. F. Reddy for his assistance in preparing the TEM specimens. This work was supported by the US Department of Energy, Basic Energy Sciences, Materials Science, under Contract W-31-109-Eng-38.

References

1. A. H. CLAUER, M. S. SELTZER and B. A. WILCOX, *J. Mater. Sci.* **6** (1971) 1379.
2. A. DOMINGUEZ-RODRIGUEZ, M. SANCHEZ, R. MARQUEZ, J. CASTAING, C. MONTY and J. PHILIBERT, *Phil. Mag.* **A46** (1982) 411.
3. J. L. ROUTBORT, *Acta Metall.* **30** (1982) 663.
4. *Idem*, in "Defect Properties and Processing of High-Technology Nonmetallic Materials", edited by J. H. Crawford, Y. Chen and W. A. Sibley (North-Holland, New York, 1984) p. 93.
5. K. C. GORETTA, J. L. ROUTBORT and T. A. BLOOM, *J. Mater. Res.* **1** (1986) 124.
6. V. KRISHNAMACHARI, *J. Mater. Sci.* **11** (1976) 1031.
7. J. CASTAING, A. DOMINGUEZ-RODRIGUEZ and C. MONTY, in "Deformation of Ceramic Materials II", edited by R. E. Tressler and R. C. Bradt (Plenum, New York, 1984) p. 141.
8. V. W. NEHRING, J. R. SMYTH and T. D. MCGEE, *J. Amer. Ceram. Soc.* **60** (1977) 328.
9. J. L. ROUTBORT, J. CASTAING and K. C. GORETTA, *ibid* **69** (1986) C114.
10. K. C. GORETTA, PhD thesis, Illinois Institute of Technology, Chicago, Illinois (1986).
11. W. R. CANNON and T. G. LANGDON, *J. Mater. Sci.* **18** (1983) 1.
12. J. CABRERA-CAÑO, A. DOMINGUEZ-RODRIGUEZ, R. MARQUEZ, J. CASTAING and J. PHILIBERT, *Phil. Mag.* **A46** (1982) 397.
13. K. C. GORETTA and J. L. ROUTBORT, in Proceedings of Materials Research Society 1985 Fall Meeting, Boston Massachusetts, 1985, in press.
14. V. KRISHNAMACHARI and M. R. NOTIS, *Acta Metall.* **25** (1977) 1307.
15. J. CASTAING and A. DOMINGUEZ-RODRIGUEZ, presented at International Conference on Defects in Insulating Crystals, Salt Lake City, Utah, 1984.
16. M. S. JAGADEESH and M. S. SEEHRA, *Solid State Commun.* **37** (1981) 369.
17. V. KRISHNAMACHARI, M. R. NOTIS and D. M. SHAH, *J. Mater. Sci.* **12** (1977) 666.
18. O. D. SHERBY and P. M. BURKE, *Prog. Mater. Sci.* **13** (1968) 325.
19. G. STREB and B. REPPICH, *Phys. Status Solidi (a)* **16** (1973) 493.

Received 27 January
and accepted 14 March 1986